Islamic Azad University
Mashhad Branch

Daneshvar Saein / Iranian Journal of Earth Sciences 9 (2017) / 64-72

Delineation of enriched zones of Mo, Cu and Re by concentration-volume fractal model in Nowchun Mo-Cu porphyry deposit, SE Iran

Lili Daneshvar Saein

Department of Geology, Payame Noor University of Tehran, Iran

Received 12 August 2015; accepted 3 January 2017

Abstract

The purpose of this study is to identify the enriched zones of Cu, Mo and Re in Nowchun Mo-Cu porphyry deposit (SE Iran) based on subsurface data and using of concentration–volume (C–V) fractal model. The C-V model illustrates four, five and three geochemical zones for Mo, Cu and Re distributions respectively. The main mineralization for Mo, Cu and Re commence from 251 ppm, 0.2% and 2238 ppb respectively, based on the C-V fractal modelling. However, elemental enriched zones contain Mo ≥ 501 ppm, Cu ≥ 0.4% and Re ≥ 4466 ppb. Based on a correlation between results obtained by the C-V and geological models, the supergene enrichment zone with Cu≥ 0.4% occurs in a small area of NE part at the Nowchun deposit within chalcocite accumulation. The enriched zones for Mo and Re derived via the C-V model are located in the NE, central and SW parts of the deposit. Mo and Re enriched zones correlate with molybdenite in the deposit.

Keywords: Concentration–volume (C–V) fractal model, Mo-Cu porphyry deposit, Enriched Zones, Re, Nowchun, Iran

1. Introduction

Fractal models were established by Mandelbrot (1983), which have been comprehensively applied to geosciences in the past three decades. These models have been utilized for distinguishing geological objectives and features (Mandelbrot, 1983; Cheng, 1995, 2007; Sim et al., 1999; Shen and Zhao, 2002; Wang et al., 2011) and for separating different anomalies from background values (Cheng et al., 1994; Goncalves et al., 2001; Li et al., 2003; Ali et al., 2007; Carranza, 2008; Afzal et al., 2010; Hassanpour and Afzal, 2011), and for quantifying properties of mineralized zones and ore deposits (Turcotte, 1986; Agterberg, 1993; Cheng and Agterberg, 2009; Zuo et al., 2009; Carranza and Sadeghi, 2010; Afzal et al., 2011, 2012; 2015; 2016; Wang et al., 2011; Zuo 2011a,b; Zhao et al., 2011). Fractal models are proper approaches for separation of geochemical populations especially for enriched zones of ore elements.

Fractal models were established by Mandelbrot (1983), which have been comprehensively applied to geosciences in the past three decades. These models have been utilized for distinguishing geological objectives and features (Mandelbrot, 1983; Cheng, 1995, 2007; Sim et al., 1999; Shen and Zhao, 2002; Wang et al., 2011)
and for separating different anomalies from background values (Cheng et al., 1994; Goncalves et al., 2001; Li et al., 2003; Ali et al., 2007; Carranza, 2008; Afzal et al., 2010; Hassanpour and Afzal, 2011), and for quantifying properties of mineralized zones and ore deposits (Turcotte, 1986; Agterberg, 1993; Cheng and Agterberg, 2009; Zuo et al., 2009; Carranza and Sadeghi, 2010; Afzal et al., 2011, 2012; 2015; 2016; Wang et al., 2011; Zuo 2011a,b; Zhao et al., 2011).
Fractal models are proper approaches for separation of geochemical populations especially for enriched zones of ore elements.

In this paper, the concentration-volume (C-V) fractal model is used to distinguish the enriched zones of the Cu, Mo and Re based on borehole datasets in Nowchun Mo-Cu porphyry deposit located in SE Iran. In this analysis the fractal model is briefly presented for demonstrating the data processing involved. On the other hand, comparison between results obtained by the C-V fractal and geological models consisting of zonation, alteration and mineralography to discriminate enriched zones were carried out.

2. Concentration-volume (C-V) fractal model

The C-V fractal model, which was proposed by Afzal et al. (2011) for determination of various mineralized zones and host rocks in porphyry deposits, which is used to describe elemental spatial distributions. The model is expressed by the following equation:

$V(\rho \leq \upsilon) \propto \rho^{-a1}$; $V(\rho \geq \upsilon) \propto \rho^{-a2}$ (1)

where V (ρ≤υ) and V (ρ≥υ) demonstrate two volumes with concentration values less than or equal to and

---

*Corresponding author.
E-mail address (es): daneshvar.saein@gmail.com

greater than or equal to the contour value ρ; υ indicates the threshold value of a mineralized zone (or volume); and a1 and a2 are characteristic exponents. Elemental threshold values in this model represent boundaries between different mineralized zones and host rocks in an ore deposit. To calculate V(ρ≤υ) and V(ρ≥υ), which are the volumes enclosed by a contour level ρ in a 3D block model, the borehole data of ore element concentrations were interpolated by use of geostatistical or IDW estimation.

3. Geological setting of Nowchun deposit

The Nowchun Mo–Cu porphyry deposit is located about 65 Km south of Rafsanjan city and 4 Km of SW Sarcheshmeh copper mine as biggest Iranian copper mine, SE Iran (Fig. 1).

This deposit is situated in the SE part of Urumieh-Dokhtar Cenozoic magmatic belt which is extended 1700 Km and 150 Km wide from NW to SE Iran, as depicted in Fig. 1 (Alavi, 1994; Shahabpour, 1994;

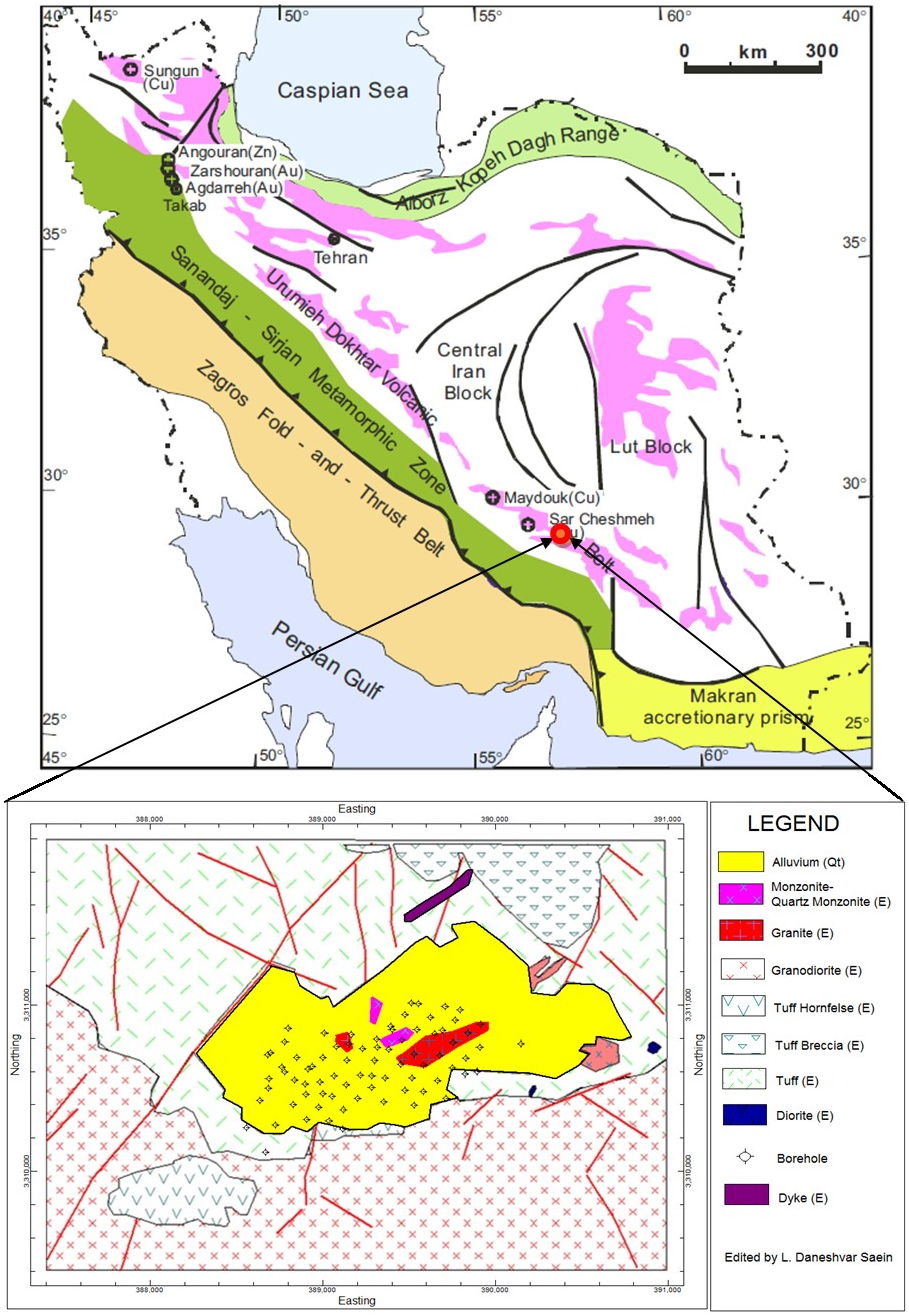

Fig. 1. Location of the Nowchun deposit and the Iranian great Cu deposits of Sar-Cheshmeh, Sungun and Maydouk at the Cenozoic–Quaternary magmatic belt of Urumieh–Dokhtar. (Modified from Stöcklin, 1968 and Daliran, 2008) whitin simplified geological map of Nowchun deposit and its boreholes locations.

Alavi, 2004; Dargahi et al., 2010; Afzal et al., 2010). This belt has been interpreted to be a subduction related Andean-type magmatic arc that has been active from the Late Jurassic to the present. The rock types of this belt are composed of voluminous tholeiitic, calcalkaline, and K-rich alkaline intrusive and extrusive rocks with associated pyroclastic and volcanoclastic successions, along the active margin of the Iranian plates (Berberian and King, 1981; Dargahi et al., 2010). The famous Iranian porphyry deposits, such as Sarcheshmeh, Sungun, Meiduk, Kahang and Darehzar have been occurred in this belt (Shahabpour, 1994; Atapour and Aftabi, 2007; Boomeri et al., 2009; Afzal et al., 2010; 2011).

There is an Eocene volcano-sedimentary complex includes granite, diorite – porphyry, tuff and rhyodacite rocks based on Yugoslavian geologists' exploration in 1972 (Fig. 1). Eocene andesitic units surround the complex and alteration zones. Porphyry Dioritic units expand in the southern part of the deposit, adjusted of the granite. Most of the Oligocene –Miocene rhyodacitic units are located in the NE part of the area. There are two major structural systems with trends of the E-W and NE-SW faults (BEOGRAD-Yugoslavia, 1972).

Alteration zones consist of potassic, phyllic, argillic and propylitic in this deposit. Argillic zone is several parts in this area but phyllic is extended in most parts of the deposit. The Cu mineral occurrences are not very abundant and consist mostly of malachite and azurite within quartz veins and veinlets contain chalcopyrite in several parts of the area. Sulfide minerals include pyrite, chalcopyrite, molybdenite, galena, sphalerite, tetrahedrite, pyrrhotite, magnetite, hematite, marcasite, chalcocite, bornite and covelite, malachite and azurite. Pyrite, chalcopyrite and molybdenite exist are numerous in this deposit.

Chalcopyrite and molybdenite were disseminated in most parts of this deposit which show that there is a big hypogene zone. Enriched copper minerals including chalcocite and covellite are low content only in the NE part of the area. Based on study by Lali faz et al. (2014), Re occurred within the molybdenites in Cu-Mo porphyry deposits of Kerman magmatic belt.

4. C-V fractal modelling in the Nowchun deposit

In this study, 20,510 samples were collected from cores at 2m intervals obtained from the 78 boreholes that were drilled in the Nowchun deposit. The samples were analyzed by the ICP-MS method for elements relating to Cu-Mo mineralization. However, 51 samples were analyzed for Re in the deposit. The Mo, Cu and Re concentrations were considered within this paper. The Mo, Cu and Re histograms show that their distributions are not normal in the deposit and Mo, Cu and Re averages are 190 ppm, 0.168% and 306 ppb, respectively (Fig. 2).

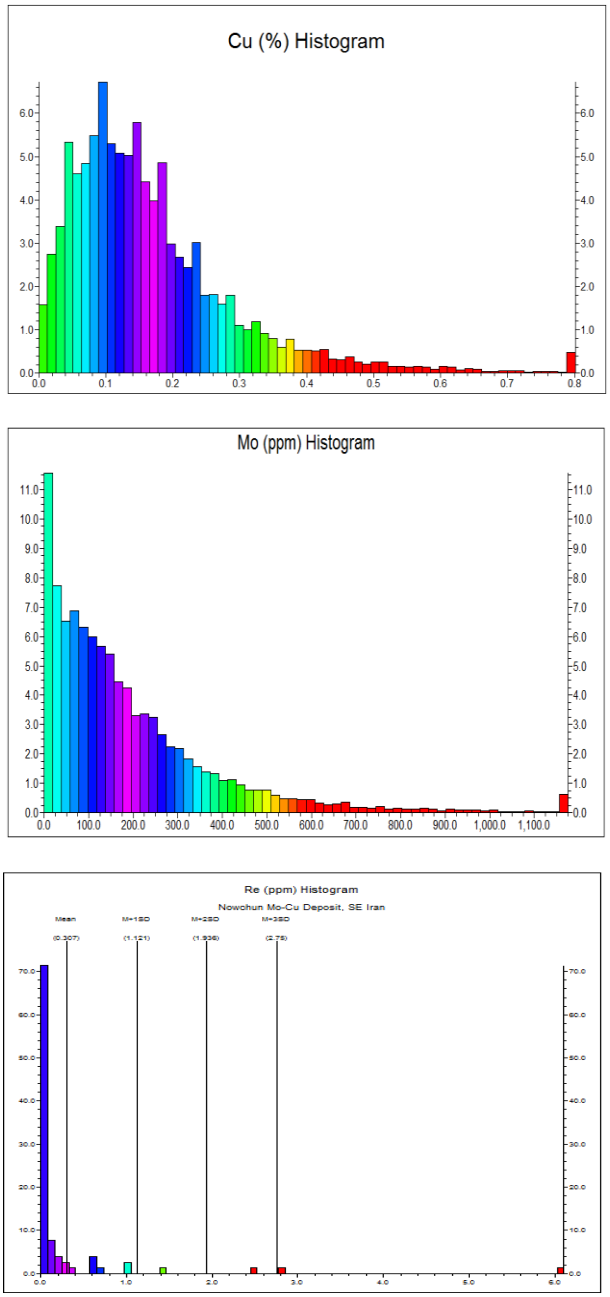

Fig. 2. Cu, Mo and Re histograms

The experimental variograms for Mo and Cu were created by SGeMS software as depicted in Fig. 3. Cu and Mo ranges are 200 m and 250 m based on their variograms. The project dimensions are 1400 m ×1040 m ×760 m in X, Y and Z direction and each voxel has a dimension of 20×20×10m, respectively, and the deposit was modelled with 391,776 voxels. 3D distributions of Mo and Cu were estimated with Ordinary Kriging (OK) but the distribution of Re is evaluated by IDW method based on small number for Re samples. Main mineralization in this deposit is Mo and Cu is minor ore element. Re is paragenesis of Mo in the porphyry deposits.

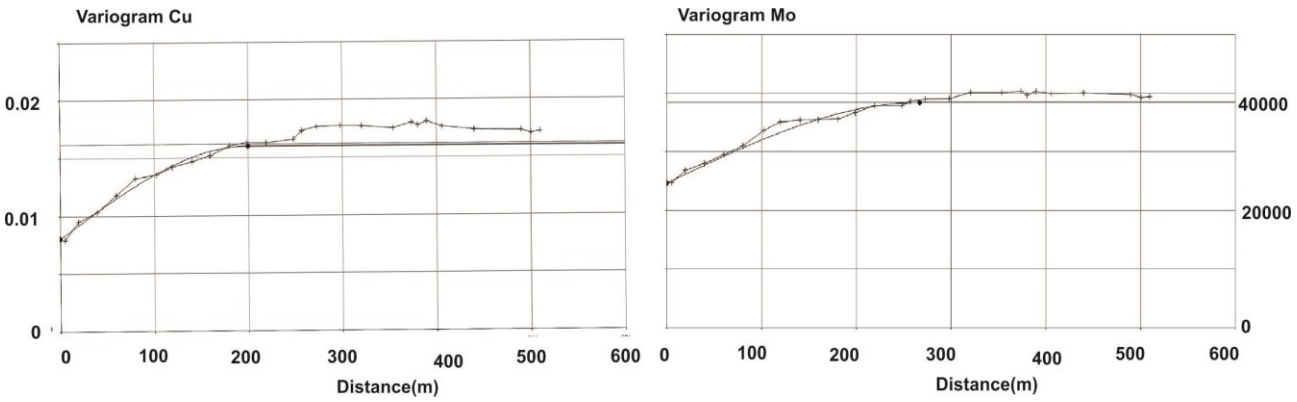

Fig. 3. Cu and Mo experimental variograms in the Nowchun deposit

Cu and Mo ranges are 200 m and 250 m based on their variograms. The project dimensions are 1400 m ×1040 m ×760 m in X, Y and Z direction and each voxel has a dimension of 20×20×10m, respectively, and the deposit was modelled with 391,776 voxels. 3D distributions of Mo and Cu were estimated with Ordinary Kriging (OK) but the distribution of Re is evaluated by IDW method based on small number for Re samples. Main mineralization in this deposit is Mo and Cu is minor ore element. Re is paragenesis of Mo in the porphyry deposits.

Mo threshold values were identified by the C-V log–log plot which shows four geochemical populations and three threshold values corresponding to 126, 251 and 501 ppm, as depicted in Fig. 4 and Table 1. Mo enriched zone have values higher than 501 ppm based on the C-V log-log plot for Mo. The log-log plot illustrates a multifractal model for Mo which shows two phase of Mo mineralization. The Mo main mineralization begins from the second threshold which is 251 ppm in this deposit. However, Mo≤224 ppm is considered as host rock in terms of Mo distribution.

Table 1. Mo and Cu thresholds calculated by C-V fractal model in the Nowchun deposit

Geochemical population	Mo (ppm) threshold value	Range Mo (ppm)	Cu (%) threshold value	Range Cu (%)
First	-	-	-	<0.06
Second	-	<126	0.06	0.06-0.2
Third	126	126-251	0.2	0.2-0.32
Fourth	251	251-501	0.32	0.32-0.4
Fifth	501	>501	0.4	>0.40

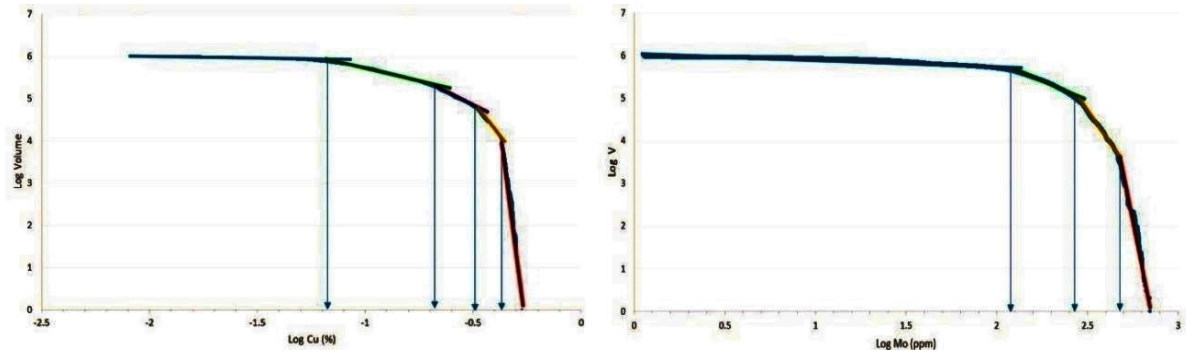

Fig. 4. C-V log-log plots for Cu and Mo

In accordance with the application of the C-V fractal model for Cu, there are five populations with four breakpoints according to the log-log plot corresponding to 0.06%, 0.2%, 0.32% and 0.4% in the deposit (Fig. 4 and Table 2). The Cu log-log plot depicts a multifractal model for Cu mineralization same as Mo. The first threshold of 0.06% characterizes the start of the Cu mineralization in the deposit and the range of Cu concentrations <0.2% is considered as host rocks. The second threshold value of Cu is 0.2% where the main Cu mineralization starts from. The range of Cu values > 0.4% demonstrates an enriched zone for Cu. Main mineralization commences from 0.4% Cu values and includes main part of hypogene and supergene enrichment zones.

Based on C-V fractal modelling for Re, there are three population and two breakpoints regarding to 2238 and 4466 ppb. Main Re mineralization commences from the first threshold which is 2238 ppb. The Re concentrations higher than 4466 ppb illustrate enriched zone for Re based on the fractal modelling. 3D distribution models of the elements have been generated by RockWorks software packages in order to prepare the basic fundamentals for the C-V fractal model. Based on the C-V fractal model, supergene enrichment zone with Cu>0.4% is very small and located in the NE part of the deposit. Hypogene zone with Cu≥ 0.32% is disposed in a SW-NE trend, as depicted in Fig. 5. According to the C-V fractal model of Mo, enriched zone with Mo higher than 501 ppm is situated in small parts of the central and SW parts of the deposit. The hypogene zone with 251-501 ppm Mo values occur in the SW-NE trend of the deposit (Fig 6). Re concentrated areas are located in eastern and NE parts of the deposit, especially Re enriched zone with Re > 4466 ppb, as depicted in Fig. 7.

Table 2. Re thresholds calculated by C-V model in the Nowchun deposit

Geochemical population	Re (ppb) threshold value	Range Re (ppb)
First	-	<2238
Second	2238	2238-4466
Third	4466	>4466

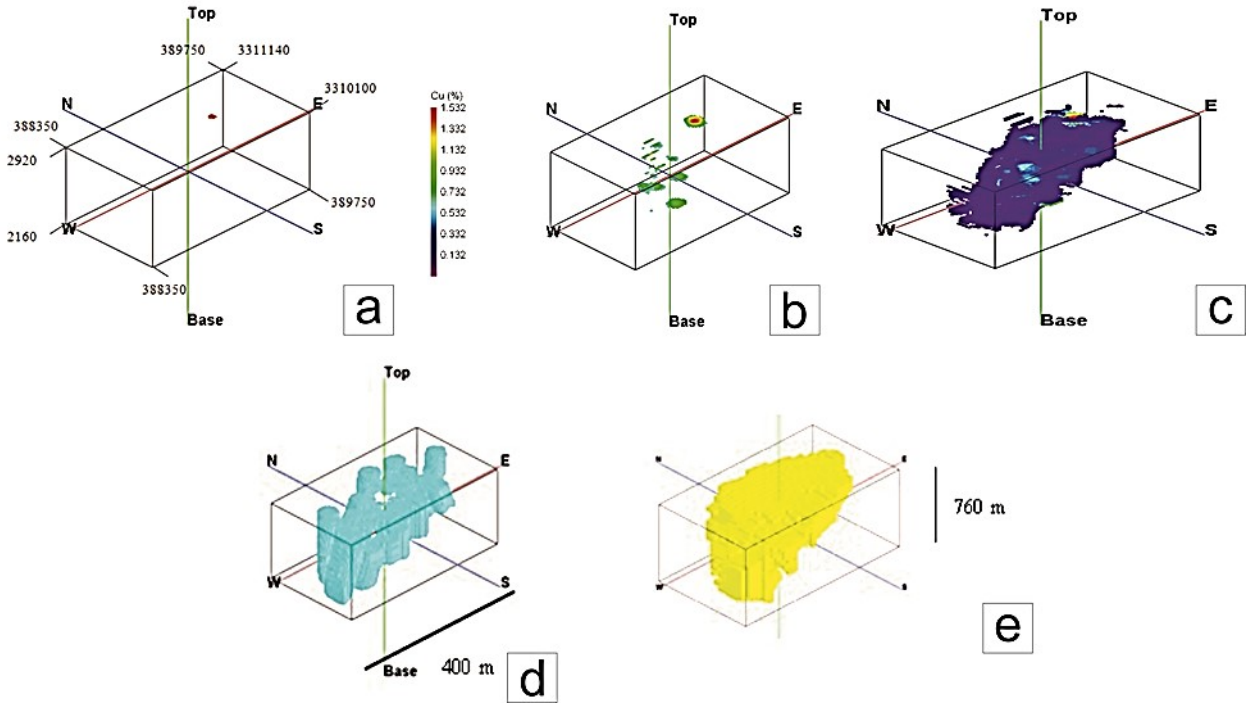

Fig. 5. Cu populations based on C-V model: supergene enrichment zone for Cu (a), hypogene zone with 0.32%<Cu<0.4% (b), low grade hypogene zone with 0.2%<Cu<0.32% (c), host rocks (d) and hypogene geological zone including pyrites and chalcopyrites

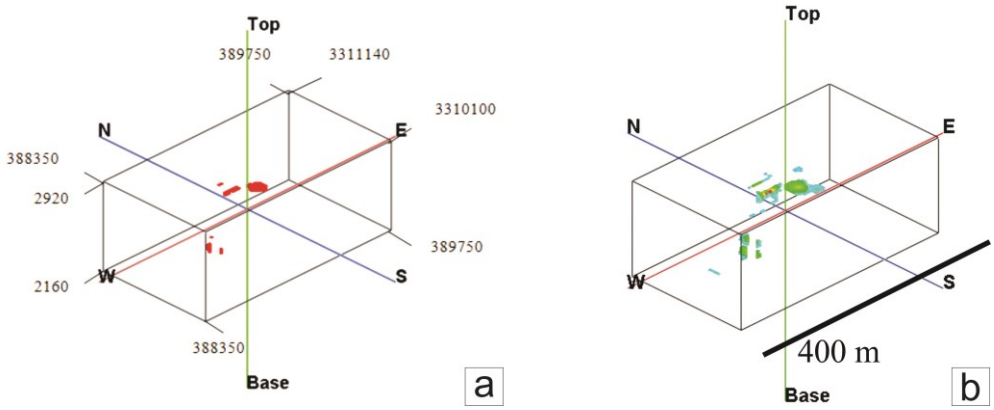

Fig. 6. Mo populations based on C-V model: Mo enriched zone with Mo> 501 ppm (a) and hypogene zone with 251<Mo<501 ppm (b)

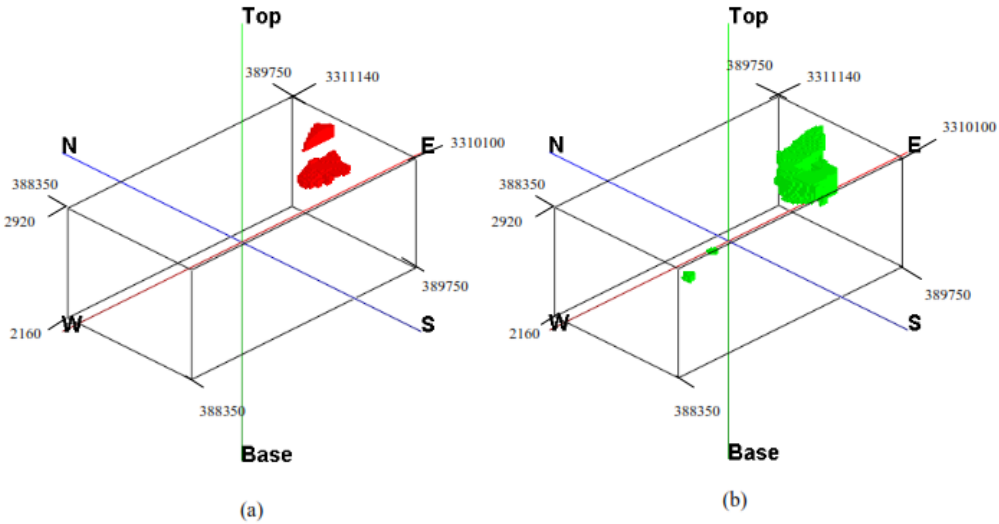

Fig. 7. Re populations based on C-V model: Re enriched zone with Re> 4466 ppb (a) and zone with 2238<Re<4466 ppb (b)

5. Comparison of C–V modelling with geological models

Elemental enriched zones obtained by the C-V modelling are compared and correlated with the 3D geological models of this deposit which generated by RockWorks™ v. 15 software and subsurface data collected from drillcores. These data include collar coordinates of drillcores, azimuth and dip (orientation), mineralography and geological zonation in according to geological logging of drillcores.

The supergene enrichment zone defined by the C-V modelling (0.4≥ Cu values) is located in a small area which is well correlated by chalcocite and supergene enrichment zone derived via geological model in the NE part of the deposit (Fig. 8). The chalcocite is seen only in NOC_16, as depicted in Fig. 8.

This is only part of supergene enrichment zone with geological evidence. However, enriched zones for Mo and Re correlate with molybdenite distribution model, as illustrated in Fig. 9. It is a geological evidence for validation of the C-V modelling results because Re is concentrated in molybdenite (Guilbert and Park, 1986; Pirajno, 2009). Moreover, the enriched zones of the Mo and Re have a good correlation with hypogene zone obtained by geological model (Fig. 9). Based on geological study, hypogene zone is extended in all parts of the deposit.

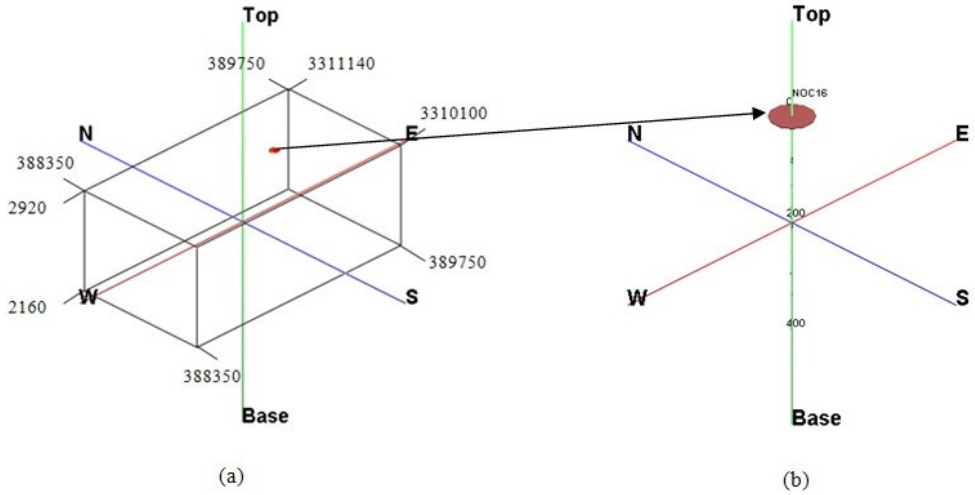

Fig. 8. Comparison and correlation between supergene enrichment zone resulted by C-V modeling and chalcocite distribution in NOC_16

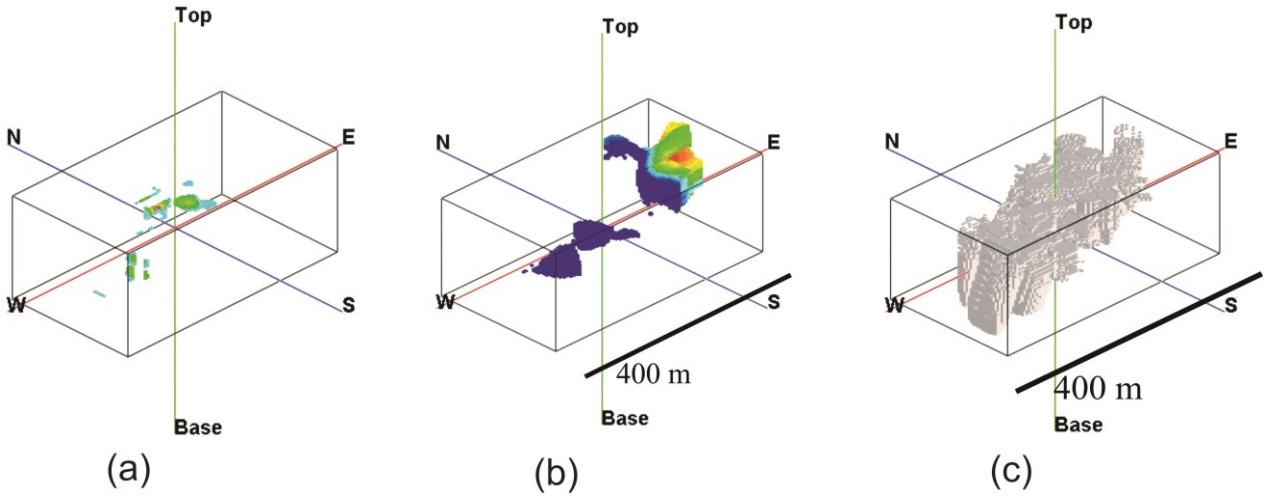

Fig. 9. Correlation between Mo (a) and Re (b) enriched zones resulted from C-V modeling with Molybdenite model (c) derived via geological model

6. Conclusion

In this paper, the C-V fractal model was used to delineate Mo, Cu and Re mineralized zones in the Nowchun Mo-Cu porphyry deposit, SE Iran. Based on the results obtained from the C-V fractal model, the last threshold values for Mo, Cu and Re are 501 ppm, 0.4% and 4466 ppb, respectively. Supergene enrichment zone have Cu≥0.4% which is very small and situated in the NE part of the deposit. The Mo enriched zones are small parts in the central and SW parts of the deposit also Re enriched zone is located in the NE part of the deposit. However, thresholds for enriched zones of Mo, Cu and Re are 501 ppm, 0.4% and 2238 ppb, respectively.

According to the correlation between results of the C-V fractal model and geological data, the enriched zones obtained by the C-V fractal model have a proper correlation with the mineralographical model. The Cu supergene enrichment zone correlates with chalcocite mineral in the NE part of the deposit. Correlation between the Mo-Re enriched zones derived via the C–V model and mineralographical characteristics shows that the Mo-Re enriched zone has a high correlation with the molybdenite accumulations in the Nowchun deposit. Moreover, the Mo-Re enriched zones associate with the hypogene zone derived via geological model.

Acknowledgments

The author thanks the kind help and authorization for release of exploration data set of Nowchun deposit to National Iranian Copper Industries Co. (NICICO) especially Mr. Esfahanipour, Mr. Sabzalian, Mr. Maghami, Mr. Khosrojerdi, Mr. Taghizadeh and Mr. Yousefian. The author wish to acknowledge the efforts of Dr. Peyman Afzal for improving the quality of the paper.

References

Afzal P, Eskandarnejad Tehrani M, Ghaderi M, Hosseini MR (2016) Delineation of supergene enrichment, hypogene and oxidation zones utilizing staged factor analysis and fractal modeling in Takht-e-Gonbad porphyry deposit, SE Iran, *Journal of Geochemical Exploration* 161: 119-127.

Afzal P, Fadakar Alghalandis Y, Khakzad A, Moarefvand P, Rashidnejad Omran N (2011) Delineation of mineralization zones in porphyry Cu deposits by fractal concentration-volume modeling, *Journal of Geochemical Exploration* 108: 220–232.

Afzal P, Fadakar Alghalandis Y, Khakzad A, Moarefvand P, Rashidnejad Omran N, Asadi Haroni H (2012) Application of power-spectrum–volume fractal method for detecting hypogene, supergene enrichment, leached and barren zones in Kahang Cu porphyry deposit, Central Iran. *Journal of Geochemical Exploration* 112: 131-138.

Afzal P, Khakzad A, Moarefvand P, Rashidnejad Omran N, Esfandiari B, Fadakar Alghalandis Y (2010) Geochemical anomaly separation by multifractal modelling in Kahang (Gor Gor) porphyry system, Central Iran, *Journal of Geochemical Exploration* 104: 34–46.

Afzal P, Madani N, Shahbeik Sh, Yasrebi AB (2015) Multi-Gaussian kriging: a practice to enhance delineation of mineralized zones by Concentration–Volume fractal model in Dardevey iron ore deposit, SE Iran, *Journal of Geochemical Exploration* 158: 10–21.

Agterberg FP, Cheng Q, Wright DF (1993) Fractal modeling of mineral deposits. In: Elbrond, J., Tang, X. (Eds.), *24th APCOM symposium proceeding*, *Montreal*, *Canada*, pp. 43–53.

Alavi M (1994) Tectonic of Zagros orogenic belt of Iran: new data and interpretations, *Tectonophysics* 229: 211–238.

Alavi M (2004) Regional stratigraphy of the Zagros folded-thrust belt of Iran and its proforeland evolution, *American Journal of Science* 304: 1-20.

Ali Kh, Cheng Q, Zhijun C (2007) Multifractal power spectrum and singularity analysis for modelling stream sediment geochemical distribution patterns to identify anomalies related to gold mineralization in Yunnan Province, South China, *Geochemistry: Exploration, Environment, Analysis* 7 (4): 293–301.

Atapour H, Aftabi A (2007) The geochemistry of gossans associated with Sarcheshmeh porphyry copper deposit, Rafsanjan, Kerman, Iran: Implications for exploration and the environment, *Journal of Geochemical Exploration* 93: 47-65.

Baldwin JA, Pearce JA (1982) Discrimination of productive and nonproductive porphyritic intrusions in the Chilean Andes. *Economic Geology* 77: 664–674.

BEOGRAD-Yugoslavia (1972) Explorations for copper in Nowchon area institute Geological and mining exploration, *National Iranian Copper Industries Co. (NICICO)*, 286 p.

Berberian M, King GC (1981) Towards a paleogeography and tectonic evolution of Iran, *Canadian Journal of Earth Sciences* 18: 210–265.

Berger BR, Ayuso RA, Wynn JC, Seal RR (2008) Preliminary Model of Porphyry Copper Deposits. *USGS*, Open-File Report. 1321 pp.

Boomeri M, Nakashima K, Lentz DR (2009) The Miduk porphyry Cu deposit, Kerman, Iran: A geochemical analysis of the potassic zone including halogen element systematics related to Cu mineralization processes, *Journal of Geochemical Exploration* 103 (1): 17-19.

Cannell J, Cooke DR, Walshe JL, Stein H (2005) Geology, mineralization, alteration, and structural evolution of the El Teniente porphyry Cu-Mo deposit, *Economic Geology* 100: 979–1003.

Carranza EJM (2008) Geochemical anomaly and mineral prospectivity mapping in GIS. *Handbook of Exploration and Environmental Geochemistry, Vol. 11. Elsevier, Amsterdam*. 351 pp.

Carranza EJM, Sadeghi M (2010) Predictive mapping of prospectively and quantitative estimation of undiscovered VMS deposits in Skellefte district (Sweden), *Ore Geology Reviews* 38: 219–241.

Cheng Q. (1995) The perimeter-area fractal model and its application to geology, *Mathematical Geology* 27: 69–82.

Cheng Q (1999) Spatial and scaling modelling for geochemical anomaly separation, *Journal of Geochemical Exploration* 65 (3): 175–194.

Cheng Q, 2007. Mapping singularities with stream sediment geochemical data for prediction of undiscovered mineral deposits in Gejiu, Yunnan Province, China. *Ore Geology Review* 32: 314–324.

Cheng Q, Agterberg FP (2009) Singularity analysis of ore-mineral and toxic trace elements in stream sediments, *Computers and Geosciences* 35 (2): 234–244.

Cheng Q, Agterberg FP, Ballantyne SB (1994) The separation of geochemical anomalies from background by fractal methods, *Journal of Geochemical Exploration* 51: 109–130.

Cox D, Singer D (1986) Mineral deposits models, *U.S. geological survey bulletin*. 1693 pp.

Daliran F (2008) The carbonate rock-hosted epithermal gold deposit of Agdarreh, Takab geothermal field, NW Iran—hydrothermal alteration and mineralization, *Mineralium Deposita* 43: 383–404.

David M (1977) *Geostatistical Ore Reserve Estimation, Amsterdam: Elsevier*, 283 p.

Dargahi S, Arvin M, Pan Y, Babaei A (2010) Petrogenesis of post-collisional A-type granitoids from the Urumieh–Dokhtar magmatic assemblage, Southwestern Kerman, Iran: Constraints on the Arabian–Eurasian continental collision, *Lithos* 115: 190-204.

Goncalves MA, Mateus A, Oliveira V (2001) Geochemical anomaly separation by multifractal modeling, *Journal of Geochemical Exploration* 72: 91–114.

Guilbert JM, Park CF (1986) *The geology of ore deposits: New York, W. H. Freeman*, 985 p.

Hassanpour Sh, Afzal P (2011) Application of concentration-number (C-N) multifractal modelling for geochemical anomaly separation in Haftcheshmeh porphyry system, NW Iran, *Arabian Journal of Geosciences* 6: 957–970.

Lali faz S, Shafiei B, Shamanian GhH, Taghizadeh H (2014) Metallogenic and Exploratory Approaches of Rhenium (Re) and Osmium (Os) Isotopic Data in Kerman Porphyry Copper Deposits, *Geosciences* 24: 245-252 (In Persian with English Abstract).

Li C, Ma T, Shi J (2003) Application of a fractal method relating concentrations and distances for separation of geochemical anomalies from background, *Journal of Geochemical Exploration* 77: 167–175.

Lowell JD, Guilbert JM (1970) Lateral and vertical alteration-mineralization zoning in porphyry ore deposits, *Economic Geology* 65: 373–408.

Mandelbrot BB (1983) *The Fractal Geometry of Nature. W. H. Freeman, San Fransisco*. 468 pp.

Melfos V, Vavelidis M, Christo des G, Seidel E (2002) Origin and evolution of the Tertiary Maronia porphyry copper–molybdenum deposit, Thrace, Greece, *Mineralium Deposita* 37: 648–668.

Pirajno F (2009) *Hydrothermal processes and mineral system: Vol. 1, Springer*, 1250 p.

Schwartz GM (1947) Hydrothermal alteration in the "porphyry copper" deposits, *Economic Geology* 42: 319–352.

Shahabpour J (1994) Post-mineral breccia dyke from the Sar-Cheshmeh porphyry copper deposit, Kerman, Iran, *Exploration and Mining Geology* 3: 39–43.

Shen W, Zhao P (2002) Theoretical study of statistical fractal model with applications to mineral resource prediction, *Computers and Geosciences* 28: 369–376.

Sillitoe RH, Gappe IM (1984) Philippine porphyry copper deposits: geologic setting and characteristics, *Common coordination joint resource (CCOP)* 14: 1-89.

Sillitoe RH (1997) Characteristics and controls of the largest porphyry copper–gold and epithermal gold deposits in the circum-Pacific region, *Australian Journal of Earth Science* 44: 373–388.

Sim BL, Agterberg FP, Beaudry C (1999) Determining the cut off between background and relative base metal contamination levels using multifractal methods, *Computers and Geosciences* 25: 1023–1041.

Stöcklin J (1968) Structural history and tectonics of Iran: a review, *Am Assoc Pet Geol. Bull.* 52: 1229–1258.

Turcotte DL (1986) A fractal approach to the relationship between ore grade and tonnage, Economic Geology 18, 1525–1532.

Wang QF, Deng J, Liu H, Wang Y, Sun X, Wan L (2011) Fractal models for estimating local reserves with different mineralization qualities and spatial variations, *Journal of Geochemical Exploration* 108: 196–208.

Zou R, Cheng Q, Xia Q (2009) Application of fractal models to characterization of vertical distribution of geochemical element concentration, *Journal of Geochemical Exploration* 102 (1): 37–43.

Zou R (2011a) Identifying Geochemical Anomalies Associated with Cu and Pb-Zn Skarn Mineralization Using Principal Component Analysis and Spectrum-Area Fractal Modelling in the Gangdese Belt, Tibet (China), *Journal of Geochemical Exploration* 111: 13-22.

Zou R (2011b) Decomposing of mixed pattern of arsenic using fractal model in Gangdese belt, Tibet, China. *Applied Geochemistry* 26: 271-273.

Zhao J, Chen S, Zou R, Carranza EMJ (2011) Mapping complexity of spatial distribution of faults using fractal and multifractal models: vectoring towards exploration targets, *Computers & Geosciences* 37: 1958-1966.